# RESEARCH ON ENERGY MANAGEMENT FOR HYBRID-POWERED VESSELS BASED ON NEURAL NETWORKS AND MODEL PREDICTIVE CONTROL

Dongping REN[1]*, Wenwen LIU[2], Jiangfeng ZHU[3], Wei CHEN[4], Xiaojun GUO[5]

*Hybrid-powered ships can effectively improve energy efficiency and reduce emissions by reasonable distribution of the output power among diesel engines and battery packs. To solve the problems of inaccurate physical models and poor adaptability of existing hybrid-powered ship models under complex operating conditions, this study proposed an intelligent energy management strategy (EMS) integrating back propagation (BP) neural network with model predictive control (MPC). Firstly, reverse modeling method was employed to develop the hybrid power system energy model; secondly, adaptive moment estimation (Adam) algorithm was applied to optimize the weights of BP neural network and a parallel compensation prediction framework was developed to enhance the accuracy of prediction and adaptive capacity of the model; finally, the designed Adam-BP-MPC EMS was verified by multi-condition simulations. Simulation results confirmed that the strategy outperforms traditional MPC in energy conservation and carbon reduction across diverse operating conditions. The Adam-BP-MPC strategy achieves rational allocation of output power between diesel engines and battery packs by virtue of the neural network's online learning and error compensation mechanisms, which effectively reduces carbon emissions and significantly elevates the overall performance of the energy management system. This error prediction-integrated control method provides an effective solution for the optimal control of hybrid-powered ships under real navigation conditions, and its integration of BP neural network and MPC offers a promising paradigm for power distribution optimization in marine hybrid power systems to cut down emissions.*

**Keywords:** Hybrid power ships; Energy management strategy; Back propagation neural network; Model predictive control

## 1. Introduction

With the intensification of global climate change and environmental protection requirements, the International Maritime Organization has set preliminary emission reduction targets urging the reduction of greenhouse gas

[1*] Naval Logistics Academy, Tianjin, China, e-mail: 1419863531@qq.com
[2] Shanghai Fives Intelligent Technology Co., Ltd., Tianjin, China, email: liuwenwen0412@163.com
[3] Naval Logistics Academy, Tianjin, China, email: zhanghuzhujiangfeng@126.com
[4] Naval Logistics Academy, Tianjin, China, email: xianghaiqianxing@126.com
[5] Naval Logistics Academy, Tianjin, China, email: 857993196@qq.com

(GHG) emissions from ships by at least 50% by 2050 compared to that in 2008 [1]. Hybrid ships provide extraordinary advantages in realizing energy efficiency and decreasing environmental pollution [2]. They can flexibly perform energy conversion among various energy forms based on their existing operational requirements and the optimized configuration and management of this energy are critical for achieving the energy-saving and emission-reduction objectives of hybrid ships [3, 4].

Currently, three types of energy management strategies are available, i.e., rule-based, optimization-based, and intelligent method-based strategies [5-7]. Rule-based energy management strategies are highly effective and have high response speeds; but in practical applications, rule parameters need laborious calibration and adjustment steps to realize the required energy scheduling objectives. Therefore, designing such strategies is time-consuming and vessel-specific and relies on the actual navigation situations of the ship [6,8]. Optimization-based energy management strategies includes establishing mathematical models of the ship and application of optimization algorithms to seek optimal control. This method enjoys from good energy management effects and clear objectives and is the main energy management development approach for diesel-electric ships. Some researchers have applied global optimization control methods for energy management to obtain optimal power distribution; however, this method mainly relies on complete navigation data of the ship and mostly optimizes control objectives in an offline manner, which is especially suitable for ships with fixed working conditions and routes [9,10]. Machine learning algorithms [11-16] utilize operational data to train energy management strategies, but they suffer from limitations such as poor generalization performance, large data volumes, and high experimental costs. Balancing the optimization performance and real-time performance in energy management strategies for hybrid ships is a difficult research topic.

Model predictive control (MPC)-based energy management strategy (EMS) achieves online local optimal control through and receding horizon optimization state feedback to address constrained optimization problems within the prediction horizon [17,18]. Banaei [19] developed a stochastic MPC-based EMS for all-electric ships consisting of fuel cells, batteries, and shore power systems, improving adaptability to load fluctuations under uncertain sea conditions. Vafamand [20] proposed an improved MPC-based energy scheduling method for pure electric ferries to enhance the stability of ship hybrid systems. However, MPC-based EMS suffers from high computational complexity and strong model dependency. Also, prediction bias occurs when disturbed by external environments or parameter drifts, affecting energy allocation.

This research took hybrid-powered ships consisting of lithium battery packs and dual diesel generator sets as the research object to minimize total GHG emissions considering fuel and electricity consumptions. The developed method

proposed a BP-MPC-based control strategy and the obtained results were compared with those obtained from the conventional MPC control strategy to verify the effectiveness of the proposed method, providing new insights for ship energy management.

## 2. Energy Flow Modeling in Hybrid Power Systems

Fig. 1 illustrates the structural composition of the developed hybrid power system, which was divided into power supply and load demand sides. The power supply side included a lithium battery pack and two diesel generators and the load demand side was consisted of propulsion and daily load powers, where the propulsion load power included a propulsion motor, a reduction gearbox, and a propeller. Fig. 2 shows the signal flow diagram of the backward-facing simulation, where signals were transmitted from energy demand components to energy generation components. In the figure, the expected speed $v$ was inserted into the longitudinal dynamics model of the ship to calculate the thrust $T$ required for its navigation. Considering the propeller and the reducer, the torque $T_m$ and required output rotational speed $\omega_m$ of the drive motor as well as the input power $P_m$ required by the drive motor were calculated. Combined with other electrical power sources $P_s$ of the ship, the power required by the power grid of the ship was considered to be $P_m + P_s$. Then, power distribution was performed using EMS, such that that diesel the two generator sets and battery pack provided $P_{G1}$, $P_{G2}$, and $P_{bat}$ powers, respectively. Finally, EMS was evaluated based on GHG emissions.

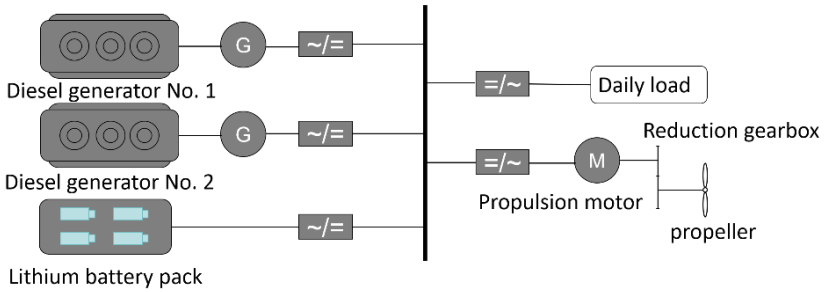


Fig. 1. Schematic diagram of the hybrid power system

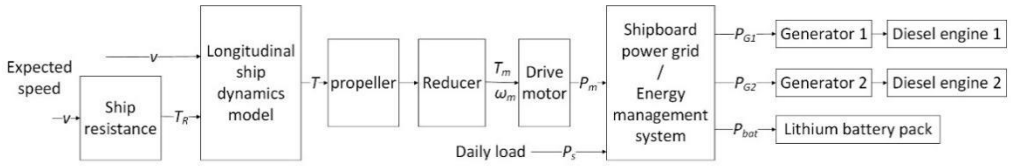


Fig. 2. Backward simulation signal flow of the hybrid power system

### 2.1 Longitudinal mechanical model

The mechanical equation for ship navigation was expressed as follows:

$$T - R_T = mv \tag{1}$$

where $T$ is propeller thrust, $R_T$ is ship resistance, $m$ is ship mass, and $v$ is ship speed.

### 2.2 Propeller model

The mathematical model of the propeller was stated as:

$$T = K_T n^2 D^4 \rho \tag{2}$$

$$Q = n^2 D^5 \rho K_Q \tag{3}$$

where $Q$ is propeller torque, $n$ is propeller rotational speed, $D$ is propeller diameter, $\rho$ is water density, $K_T$ is propeller thrust coefficient, and $K_Q$ is propeller torque coefficient.

### 2.3 Diesel generator model

Diesel generator set included a diesel prime mover and a matched generator. Fig. 3 illustrates the Map diagram of the fuel consumption rate of the diesel engine, where X-axis shows torque, Y-axis presents rotational speed, and Z-axis denotes fuel consumption rate. The working speed with lower fuel consumption rate was adopted by reading the Map diagram.

The power model of the generator was calculated as:

$$P_D = \frac{P_G}{\eta_1 \eta_2 \eta_3} \tag{4}$$

where $P_G$ is generator output power, $P_D$ is generator input power, $\eta_1$ is generation efficiency, $\eta_2$ is power distribution efficiency, and $\eta_3$ is inverter efficiency.

Diesel engine power model was stated as:

$$P_D = T_D \omega_D \tag{5}$$

where $T_D$ is diesel engine output torque and $\omega_D$ is diesel engine rotational speed.

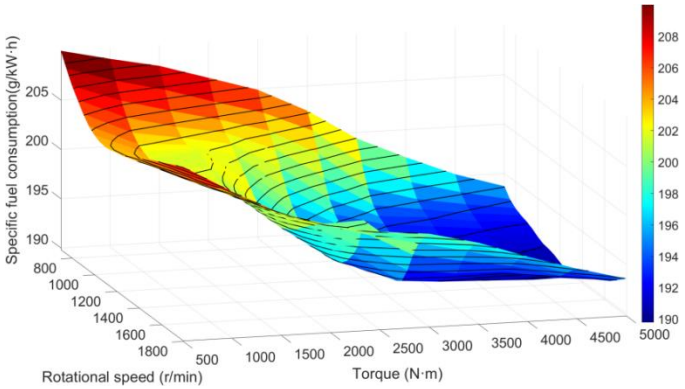


Fig. 3. Map diagram of diesel engine fuel consumption rate

## 2.4 Drive motor model

The efficiency of the propulsion motor was determined from motor efficiency Map based on the speed and torque of the motor and propulsion motor input power was calculated as:

$$P_{in} = \frac{T_m \omega_m}{\eta_m} \tag{6}$$

where $P_{in}$ is motor input power, $T_m$ is motor output torque, $\omega_m$ is motor speed, and $\eta_m$ is motor efficiency.

## 2.5 Power battery pack model

Based on Rint equivalent circuit model, the mathematical model of current was calculated as:

$$V_{oc} I_{bat} - I_{bat}^2 R_{bat} = P_{bat} \tag{7}$$

$$I_{bat} = \frac{V_{oc}}{2R_{bat}} - \sqrt{\left(\frac{V_{oc}}{2R_{bat}}\right)^2 - \frac{P_{bat}}{R_{bat}}} \tag{8}$$

The state of charge (SOC) of the battery was stated as:

$$SOC = SOC_0 - \int \frac{I_{bat} dt}{Q_{bat}} \tag{9}$$

The maximum power of the battery was calculated as:

$$P_{bat\max} = \left(V_{oc} - I_{\max} R_{bat}\right) I_{\max} \tag{10}$$

where $V_{oc}$ is battery voltage, $I_{bat}$ is battery current, $R_{bat}$ is battery internal resistance, $Q_{bat}$ is battery capacity, $P_{bat}$ is battery power, $SOC_0$ is the initial state of charge, and $I_{\max}$ is the maximum discharge current of the battery.

## 3. Energy Management Control Strategy

This research proposed an intelligent EMS (Adam-BP-MPC) that integrated Adam-optimized BP neural network with MPC. The developed approach realized the dynamic power distribution of hybrid-powered ships through a closed-loop architecture of "prediction optimization - compensation correction - rolling decision-making". Fig. 4 illustrates the overall framework of the proposed strategy.

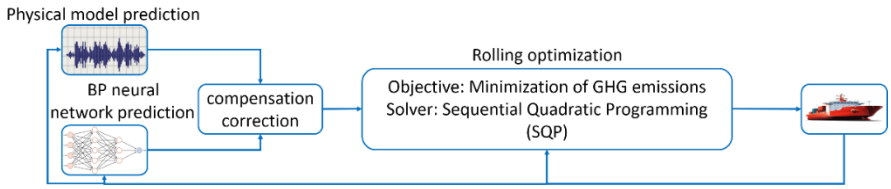


Fig. 4. The schematic diagram of the developed control strategy framework

### 3.1 Adam-improved BP Neural Network

Back propagation (BP) neural network can be employed for predictive analyses. In the scenario of ship speed-power prediction, its operation process is as follows: the ship speed entered the input layer, went through weighted summation and activation function processing of the hidden layer, and finally reached the output layer to generate the predicted power [21]. However, when using BP neural network, the initial weights and thresholds are randomly selected, which easily provides local minimum; however, training time is too long and convergence speed is low, decreasing prediction accuracy. Therefore, Adam algorithm was applied to optimize the BP neural network. The basic idea was to automatically allocate appropriate learning rates for various parameters based on first-order and second-order gradient moments, decreasing the complexity of manual parameter adjustment and the influence of noisy gradients through second-order moment estimation, making training process smoother. Parameters were updated using the following equations:

$$m_t = \beta_1 \cdot m_{t-1} + (1-\beta_1) \cdot g_t \tag{11}$$

$$v_t = \beta_2 \cdot v_{t-1} + (1-\beta_2) \cdot g_t^2 \tag{12}$$

$$\hat{m}_t = \frac{m_t}{1-\beta_1^t}, \hat{v}_t = \frac{v_t}{1-\beta_2^t} \tag{13}$$

$$\theta_t = \theta_{t-1} - \alpha \cdot \frac{\hat{m}t}{\sqrt{\hat{v}t + \varepsilon}} \tag{14}$$

where $m$ and $v$ are the first-order and second-order gradient moments, and $\hat{m}$ and $\hat{v}$ are corrected first-order and second-order gradient moments, respectively. Also, $\theta$ is neural network parameter; $g$ is gradient; and $\beta_1$ and $\beta_2$ are hyperparameters.

In Adam-BP, network weights $W$, bias $b$, and Adam parameters were first initialized. Then, the data were input for layer-by-layer calculation until the predicted value of $\hat{y}$ was obtained at output layer. Then, the mean squared error $L = \frac{1}{N}\sum_{i=1}^{N}(y_i - \hat{y}_i)^2$ and loss gradients $\nabla_W L$ $\nabla_b L$ were calculated. Finally, Adam parameters were updated.

A comparative analysis was conducted with traditional BP neural network prediction model to verify the accuracy of the developed Adam-BP neural network prediction model. The first 350 groups of data in the navigation data were adopted as training sample set and the same input and output variables were considered in both models. Both prediction models were configured as feedforward neural networks with 3 hidden layers. To ensure comparative analysis objectivity among different models, the remaining parameters were set to default values. Fig. 5 shows the prediction results obtained from the two models and Table 1 summarizes the comparison results of different indicators. Both models could capture the basic variation patterns of trend fitting in the navigation data, but Adam-BP neural network prediction curve presented a higher overlapping degree with the true values with smaller errors, indicating the advantages of the developed Adam-optimized BP neural network.

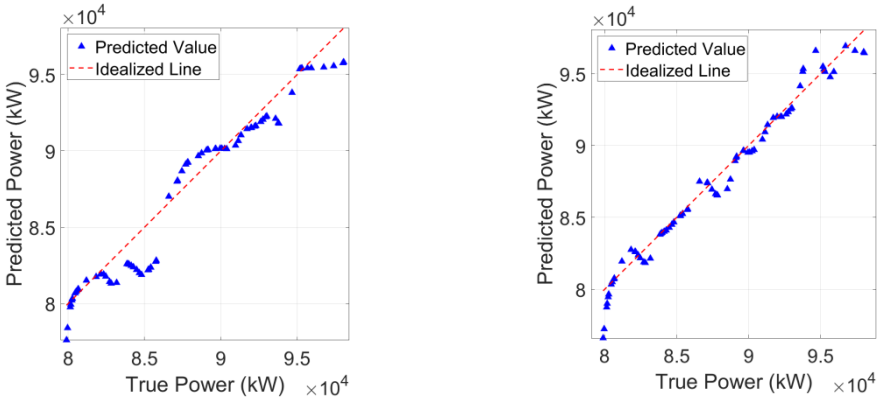


(a) BP neural network (b) Adam-BP neural network

Fig. 5. Comparison of predicted and actual powers

*Table 1*

**Comparison of Performance Indicators for the Two Models**

| Training algorithm | Hidden layer structure | Coefficient of determination ($R^2$) | Mean squared error (MSE) | Root mean squared error (RMSE) | Mean absolute error (MAE) | Mean absolute percentage error (MAPE)% |
|---|---|---|---|---|---|---|
| BP (traingdm) | 15 10 5 | 0.933 | 1846326.3 | 1358.8 | 1046.7 | 1.20 |
| Adam BP (trainscg) | 15 10 5 | 0.973 | 727674.6 | 853.0 | 580.8 | 0.67 |

### 3.2 Parallel compensation design

Traditional hybrid ship models have been constructed based on physical equations, which lack flexibility when facing complex or dynamically changing environments. However, neural networks excel in handling non-linear relationships and pattern recognition. In order to fully leverage the accuracy of the physical models and adaptive learning ability of neural networks, this research introduced a physics-neural network fusion modeling method. The developed method adopted a parallel compensation architecture, utilizing the physical model as the basic controller to handle power output and energy allocation under conventional conditions of ship operation. Under normal conditions and based on precise system parameters and dynamic equations, the physical model could achieve stable and reliable control. Neural network serves as a dynamic compensator, automatically generating compensation signals to correct the basic control output by real-time monitoring of the error between the predicted output of the physical model and the actual response of the system under complex conditions or when the prediction results of the physical model is inaccurate. This architectural design not only retains the physical essence and stability of the physical model, but also significantly

improves the adaptability of the system in complex environments through the intelligent compensation mechanism of the neural network. Parallel compensation equations were stated as:

$$u_{final} = u_{mech} + \alpha \cdot u_{NN} \tag{15}$$

$$u_{NN} = y_{real} - y_{mech} \tag{16}$$

where $u_{final}$ is final compensated output, $u_{mech}$ is physical model output, $u_{NN}$ is the compensation amount predicted by the neural network, $\alpha$ is dynamic compensation coefficient, $y_{real}$ is the measured value, and $y_{mech}$ is the value predicted by the physical model.

### 3.3 MPC control strategy

MPC is an advanced control strategy based on modern control theory, which optimizes control decisions through model prediction to effectively control complex systems. MPC-based EMS essentially involved receding horizon optimization, model prediction, and online correction. MPC solved the optimal control sequence $u^*(t_k) = \left[u^*(t_k) + u^*(t_{k+1}) +, \cdots, u^*\left(t_{k+Hp-1}\right)\right]^T$ for the energy management problem. Its calculation is based on the ship predicted speed $v(t_k) = \left[v(t_k) + v(t_{k+1}), \cdots, v\left(t_{k+Hp}\right)\right]^T$ within the prediction horizon and the current system state $x\left(t_k\right)$. MPC takes the first term $u^*\left(t_k\right)$ of this optimal control sequence as its control output. The updated system state $x\left(t_{k+1}\right)$ is fed back to the sequential quadratic programming algorithm, which enables the realization of receding horizon optimization. This research adopted SOC-based adaptive regulation to switch between the generators and the battery pack. When SOC was close to the upper limit ($SOC \geq SOC_{\max} - 5\%$), the strategy prohibited the charging of the battery and only allowed discharging, prioritizing battery discharge to decrease generator output and avoid battery overcharging. When SOC was close to the lower limit ($SOC \leq SOC_{\min} + 5\%$), the strategy prohibited the discharging of the battery and only permitted charging, forcing the generators to generate more power to charge the battery and prevent the overdischarging of the battery. When SOC was within the middle range, the battery could flexibly charge and discharge; when the required power was lower than the efficient operating lower limit of the generator ( $P_d \leq P_{G1} = 10kw$ or $P_d \leq P_{G2} = 15kw$ ), the battery supplied power independently; and when power demand surged, the battery provided auxiliary discharge.

### *3.3.1 Optimization objective*

This research aimed to minimize GHG emissions, which mainly result from the generation of carbon dioxide by fuel consumption and shore power generation. The calculation equation for GHG emissions at time $t_k$ was stated as:

$$G(t_k)=\left[E_{D1}(t_k)+E_{D2}(t_k)\right]G_{fuel}+E_{bat}(t_k)G_{ele} \tag{17}$$

where $G(t_k)$ is total GHG emissions (kg), $E_{D1}(t_k)$ and $E_{D2}(t_k)$ are the energy consumed by diesel generators 1 and 2 (kW·h), respectively, $E_{bat}(t_k)$ is the actual energy consumed by the battery (kW·h), $G_{fuel}$ is carbon dioxide emission per kWh of the energy consumed by diesel generators [kg/(kW·h)], and $G_{ele}$ is carbon dioxide emission per kWh of the energy consumed by shore power [kg/(kW·h)]. Based on the fuel consumption Map diagram presented in Section 2.3, quadratic polynomial fitting was used to determine the corresponding relationship between output power and fuel consumption rate, as illustrated in Fig. 6.

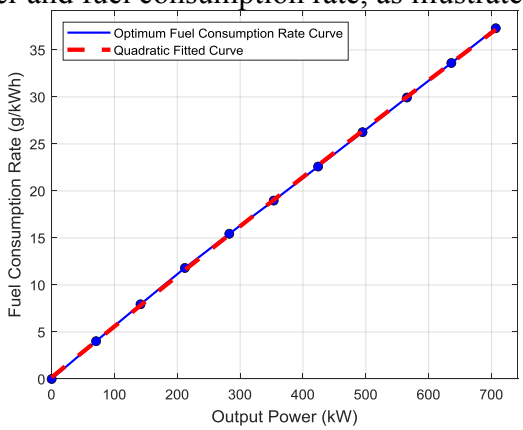


Fig. 6. Curve of optimal fuel consumption rate of diesel engine versus output power

### *3.3.2 System constraints*

Energy control strategy should meet navigation requirements as well as the demands of other loads in the ship. First, power balance equations had to be satisfied; i.e., $P_d=P_{G1}+P_{G2}+P_{bat}, P_d=P_m+P_s$. Meanwhile, both diesel generator sets and battery were within the normal operating range and the battery had to be within its upper and lower limits $\left[SOC_{\min}, SOC_{\max}\right]$. Defining system state variables as $x(t)=\left[SOC(t), P_{G1}(t), P_{G2}(t), P_{bat}(t), P_d(t)\right]^T$, the mathematical equations of system constraints were expressed as:

$$\begin{cases} P_{d\min} \le P_d(t) \le P_{d\max} \\ SOC_{\min} \le SOC(t) \le SOC_{\max} \\ 0 \le P_{G1}(t) \le P_{G1\max} \\ 0 \le P_{G2}(t) \le P_{G1\max} \\ SOC(t) \ge SOC_{\max}, P_{G1}(t) + P_{G2}(t) \ge P_{d\min} \\ SOC(t) \ge SOC_{\min}, P_{G1}(t) + P_{G2}(t) \le P_{d\max} \end{cases} \tag{18}$$

*3.3.3 MPC control process*

Prediction horizon spanned from the start time $t_0$ to the end time $t_{end}$. At any certain moment, current system variables $x(t) = \left[SOC(t), P_{G1}(t), P_{G2}(t), P_{bat}(t), P_d(t)\right]^T$ were read, while ship speed $v(t_k) = \left[v(t_k) + v(t_{k+1}), \cdots, v\left(t_{k+Hp}\right)\right]^T$ and corresponding power demand $P_d(t_k) = \left[P_d(t_k) + P_d(t_{k+1}), \cdots, P_d\left(t_{k+Hp}\right)\right]$ within the prediction horizon were loaded. Quadratic programming algorithm was applied to solve the optimal control sequence $u^*(t_k) = \left[u^*(t_k) + u^*(t_{k+1}), \cdots, u^*\left(t_{k+Hp-1}\right)\right]$ and the first term $u^*(t_k) = \left[P^*_{G1}(t_k), P^*_{G2}(t_k), P^*_{bat}(t_k)\right]$ as the output for energy distribution in the hybrid power system, with the system state $x\left(t_{k+1}\right)$ updated accordingly. The above steps were repeated until the time exceeded the end time $t_{end}$, ultimately achieving rolling optimization. Fig. 7 illustrates MPC calculation process.

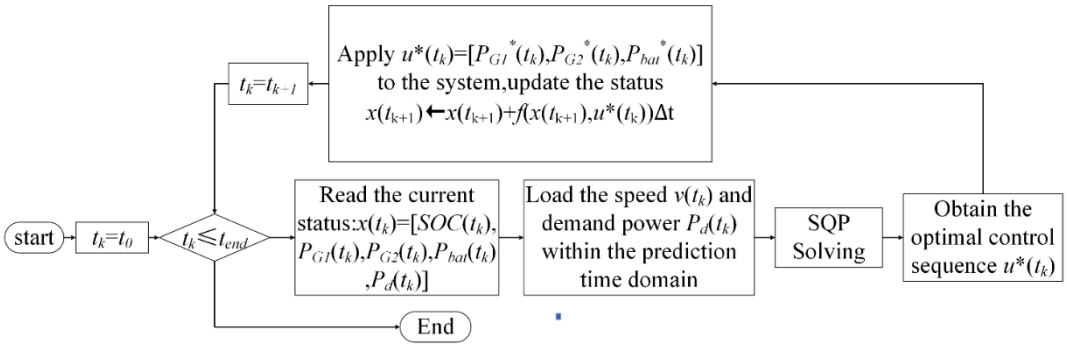


Fig. 7. MPC calculation process

## 4. Simulation result analysis

### 4.1 Simulation conditions and parameters

The navigating data of a certain ship was collected for 1 hour under two operating conditions of speed fluctuation and sudden acceleration/deceleration. Then, simulated speed curve (Fig. 8) and required power curve (Fig. 9) were generated. Table 2 summarizes simulation parameters. Before navigation, the ship charged the energy storage system through shore power device to ensure that electrical energy was used for auxiliary propulsion as much as possible during navigation, thereby improving the fuel economy of the ship. MPC prediction horizon length was $Hp = 10\,\text{min}$, control horizon length was $Hm = 2\,\text{min}$, and optimization step size was $\Delta t = 1\,\text{min}$. The simulation cycle: initial time $t_0 = 0$, end time $t_{end} = 3600\text{s}$

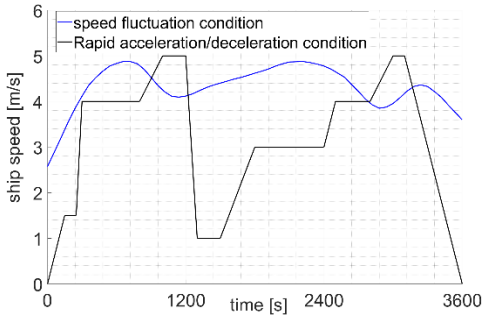


Fig. 8. Speed profile of test cycle

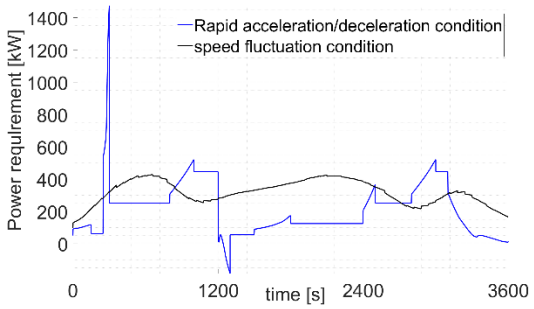


Fig. 9. Requirement power profile of test cycle

*Table 2*

**Parameters of Hybrid Ships**

| Parameter | Value |
|---|---|
| Reduction Gear Ratio | 16 |
| Transmission Efficiency of Reduction Gear /% | 98 |
| Generator Efficiency /% | 97 |
| Design Working Power of Diesel Engine 1 /KW | 283 |
| Design Working Power of Diesel Engine 2 /KW | 141 |
| Initial SOC /% | 80 |
| Battery Upper Limit SOC/% | 70 |
| Battery Lower Limit SOC/% | 30 |
| Propeller Diameter/m | 2.03 |
| Propeller Coefficient | $K_{T1}$=-0.106, $K_{T2}$=-0.3246, $K_{T3}$=0.45946, $K_{Q1}$=-0.0186, $K_{Q2}$=-0.0399, $K_{Q3}$=0.068 |
| Water Density (g/cm$^3$) | 1.025 |
| Generator Efficiency Parameters | $\eta_1$=0.97, $\eta_2$=0.99, $\eta_3$=0.98 |

### 4.2 Comparative analysis of simulation results

To verify the effectiveness of the developed Adam-BP-MPC model, simulation comparisons were performed between this strategy and MPC EMS.

*4.2.1 Ship speed fluctuation condition*

Fig. 10 illustrates the variations of instantaneous carbon emissions over time for the two EMSs under speed fluctuation conditions. It was seen from the figure that carbon emissions presented a monotonically increasing trend with operation time, which was consistent with the continuous energy consumption characteristics of the power system of the ship. Throughout the entire simulation cycle, the carbon emission curve of the proposed Adam-BP-MPC strategy always lied below that of the traditional MPC strategy, revealing its sustained advantage in controlling carbon emission. Specifically, at the end of the simulation (t = 3600 s), the total emission of the traditional MPC strategy was about 374.8 kg, while that obtained by Adam-BP-MPC strategy was about 370 kg, proving a significant emission reduction effect.

Fig. 11 shows the cumulative fuel consumption curves of the two strategies under the same operating conditions. In line with carbon emission trend, fuel consumption was continuously increased over time, yet the fuel consumption curve of the Adam-BP-MPC strategy remained below the value obtained from the traditional MPC strategy throughout the entire process. At t = 600 s, the fuel consumptions of the two strategies were similar. With further passage of time, the fuel-saving effect of Adam-BP-MPC strategy gradually became apparent. By the end of the simulation, the total fuel consumption of the traditional MPC strategy was about 92 kg, while that of Adam-BP-MPC strategy was only 80 kg, corresponding to a fuel-saving rate of about 13%. This finding revealed that Adam-BP-MPC strategy could more accurately predict the effects of speed fluctuations on power demand through online learning and adaptive adjustment capabilities of the neural network, obtaining more refined energy allocation and enhancing fuel economy.

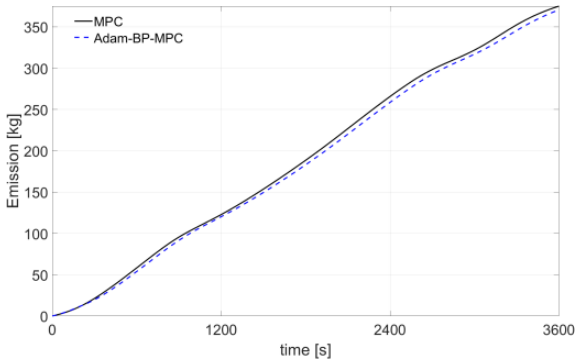


Fig. 10. Carbon emission trend chart under speed fluctuation condition

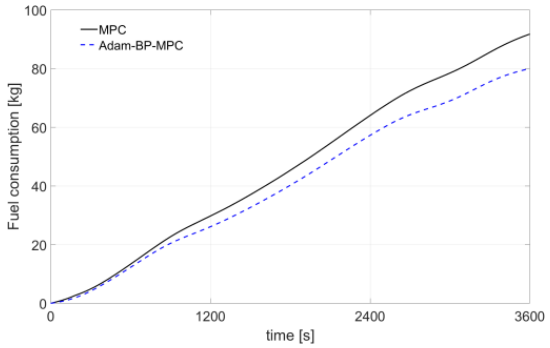


Fig. 11. Fuel consumption rate trend chart under speed fluctuation condition

### *4.2.2 Rapid acceleration/deceleration condition*

Fig. 12 shows the carbon emission performance of the two strategies under sudden acceleration and deceleration conditions. Cumulative emissions were gradually increased over time, which aligned with the dynamic operation characteristics of the ship. For $t < 1423$ s, the carbon emissions of the two strategies were roughly consistent; however, after $t > 1423$ s, the carbon emission of Adam-BP-MPC strategy was significantly lower than that of traditional MPC strategy. By the end of the simulation, the cumulative carbon emission of Adam-BP-MPC strategy was about 4 kg less than that obtained from the traditional MPC strategy. This difference revealed that under sharply changing operation conditions, Adam-BP-MPC strategy could improve the dynamic response capability of the system through neural network, more effectively realizing low-carbon operation.

Fig. 13 illustrates cumulative fuel consumption curves under sudden acceleration and deceleration conditions. Within the time range of 0–271 s, the fuel consumptions of the two strategies were comparable. During the time range of 271–646 s, the fuel consumption of Adam-BP-MPC strategy was slightly higher than that for traditional MPC, which might be due to the initial adjustment phase of the neural network in dynamic process. However, with the progress of simulation, the advantages of Adam-BP-MPC strategy gradually became prominent. By the end of the simulation, the cumulative fuel consumption of the developed approach was 14 kg lower than that of the traditional MPC strategy, denoting a significant fuel-saving effect. This proved that when facing sharply changing operation conditions, Adam-BP-MPC strategy optimized energy flow distribution through online learning, significantly enhancing the fuel economy and adaptability of the system.

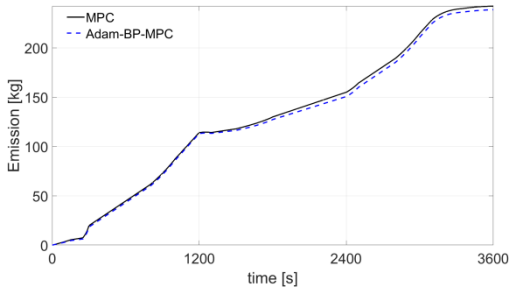


Fig. 12. Carbon emission trend chart under rapid acceleration/deceleration condition

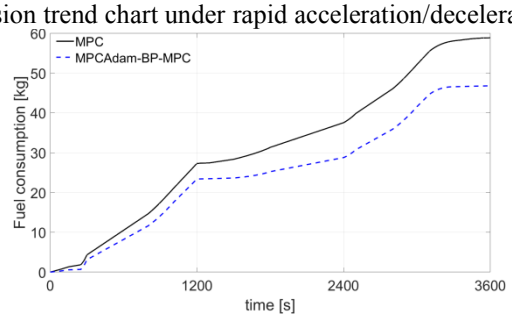


Fig. 13. Fuel consumption rate trend chart under rapid acceleration/deceleration condition

## 5. Conclusion

According to the simulation results of the two typical operating conditions mentioned above, Adam-BP-MPC strategy outperformed traditional MPC strategy in both fuel economy and carbon emission control. The advantages of the developed approach stemmed from the introduction of neural network structure, which endowed the system with adaptability to dynamic operating conditions and stronger nonlinear fitting ability, realizing more accurate and efficient energy management. This research provided valuable references for designing energy management strategies for hybrid-powered ships and demonstrated the application potential of intelligent control methods for energy conservation and emission reduction in ships.

## REFERENCES

[1] IMO (2025) Reducing Greenhouse Gas Emissions from Ships. https://www.imo.org/en/MediaCentre/HotTopics/Pages/Reducing-greenhouse-gas-emissions-from-ships.aspx.

[2] *Zahedi B, Norum L E, Ludvigsen K B* (2014) Optimized efficiency of all-electric ships by dc hybrid power systems. Journal of Power Sources. 255:341–354.

[3] *Tounsi S* (2023) Optimisation of network injected power of an innovated structure of wind turbine. Mechatronic Systems and Control. 51(2): 67-78.

[4] *Stone P, Opila D F, Park H, et al (*2015) Shipboard power management using constrained nonlinear model predictive control. 2015 IEEE Electric Ship Techno logies Symposium (ESTS). Alexandria, VA, USA: IEEE, 2015: 1-7.

[5] *Zhao X, Li W, Lin Z* (2022) Energy Management Strategies for Fuel Cell Hybrid Electric Vehicles: Classification, Comparison, and Outlook. Energy Conversion and Management. 270: 116179.

[6] *Zhang Yifeng, Wang Xihuai* (2018) Modeling and Energy Management of Hybrid Power Ships. Marine Electric & Electronic Technology. 38(7): 32-37.
[7] *Fan Ailong, Li Yongping, Yang Qiang, et al* (2024) Research on Predictive Control Method for Energy Management of Ship Hybrid Power Systems. Journal of Harbin Engineering University. 45(1): 162-173.
[8] Luna M L, Torres G A, et al (2013) Optimal management of battery and fuel cell-based decentralized generation in DC shipboard microgrids. Energies. 16(14): 1682.
[9] *Zhao* (2022) Improved Fuzzy Logic Control-Based Energy Management Strategy for Hybrid Power System of FC/PV/Battery/SC on Tourist Ship. International Journal of Hydrogen Energy. 47(16): 9719-9734.
[10] *Michalopoulos P K, Fafalis D T, Jentzsch G* (2016) A Method for Optimal Operation of Complex Ship Power Systems Employing Shaft Electric Machines. Journal of Marine Science and Engineering. 4(2): 547-557.
[11] *Lee W, Jeon J, Han P D* (2021) A Real-Time Intelligent Energy Management Strategy for Hybrid Electric Vehicles Using Reinforcement Learning. Applied Sciences. 11(16): 72759-72768.
[12] *Fortela D L B, Fremin A C, Sharp W, et al* (2023) Unsupervised Machine Learning to Detect Impending Anomalies in Testing of Fuel Economy and Emissions of Light-Duty Vehicles. Clean Technologies. 5(1): 418-435
[13] *Basel J, Ahmad A J, Abu M M* (2024) Deep Stochastic Reinforcement Learning-Based Energy Management Strategy for Fuel Cell Hybrid Electric Vehicles. Energy Conversion and Management. 301: 117973
[14] *Peksen M M* (2022) Artificial Intelligence-Based Machine Learning toward the Solution of Climate-Friendly Hydrogen Fuel Cell Electric Vehicles. Vehicles. 4(3): 663-680.
[15*] Zhang X, Ma Y, Zhang L* (2025) Virtual reality scene rendering and interaction technology based on machine learning and semi-supervised learning. Mechatronic Systems and Control. 53(4): 272-283.
[16] *Hu J P, Jian X L, Kai D, et al* (2022) Machine Learning-Based Control for Fuel Cell Hybrid Buses: From Average Load Power Prediction to Energy Management. Vehicles.4(4): 1365-1390.
[17] *He H, Wang W, Yan L H (*2021) An Improved MPC-Based Energy Management Strategy for Hybrid Vehicles Using V2V and V2I Communications. Energy. 225: 120273.
[18] *Ranjan P K, Kumar S S* (2023) A model predictive current control strategy for grid-connected single-stage boost inverter in solar photovoltaic systems. Mechatronic Systems and Control. 51(2): 86-96.
[19] *Banaei M, Bidad J, Kazerani M* (2021) Stochastic Model Predictive Energy Management in Hybrid Emission-Free Modern Maritime Vessels. IEEE Transactions on Industrial Informatics. 17(8): 5430-5440.
[20] *Vafamand N, Boudjadar J, Khooban M H* (2020) Model predictive energy management in hybrid ferry grids. Energy Reports. 6: 550-557.
[21] *Li Y, Yu Y, Hu X, et al* (2021) Vector control of permanent magnet synchronous linear motor based on improved bp neural network. Mechatronic Systems and Control. 49(2): 109-114.